Supramolecular polymerization induced by the rotation of light-driven molecular motors

Philippe Schiel,[a] Mounir Maaloum,[a] Emilie Moulin,[a] Irina Nyrkova,[b] Alexander Semenov,[b]* Damien Dattler,[a] Lou-Ann Accou,[a] Anastasia Christoulaki,[c] Eric Buhler,[c] Jean-Marie Lehn,[d] and Nicolas Giuseppone[a,e]**

[a] P. Schiel, Prof. Dr. M. Maaloum, Dr. E. Moulin, Dr. D. Dattler, L.-A. Accou, and Prof. Dr. N. Giuseppone
SAMS Research Group, Université de Strasbourg, CNRS, Institut Charles Sadron UPR 22 67000 Strasbourg, France
E-mail: maaloum@unistra.fr
E-mail: giuseppone@unistra.fr
[b] Dr. I. Nyrkova, Dr. A. Semenov
CNRS, Institut Charles Sadron UPR 22 67000 Strasbourg, France
E-mail: semenov@unistra.fr
[c] Dr. A. Christoulaki, Prof. Dr. E. Buhler, Matière et Systèmes Complexes (MSC), UMR CNRS 7057, Université Paris Cité, Bâtiment Condorcet, 75013 Paris, France
[d] Prof. Dr. J.-M. Lehn, Université de Strasbourg, Institut de Science et d'Ingénierie Supramoléculaires (ISIS), 8 allée Gaspard Monge, 67000 Strasbourg, France.
[e] Institut Universitaire de France (IUF)

Abstract

Molecular motors are capable of producing mechanical work on their environment by using their unique capacity to generate non-reciprocal autonomous motions at the nanoscale. Although their operating principles are now well understood, artificial molecular motors have yet to demonstrate their general capacity to confer novel properties on (supra)molecular systems and materials. Here we show that amphiphilic light-driven molecular motors can adsorb onto the air-water interface and form Langmuir monolayers upon compression. Under irradiation, the surface pressure isotherms of these films reveal a drastic shift toward smaller molecular areas as a consequence of their motors' activation. We explain this counterintuitive phenomenon by the rotation-induced supramolecular polymerization of the amphiphilic motors, limited by the maximal torque they can deliver, and leading to the formation of highly organized patterns. This serendipitous discovery highlights the opportunities offered by molecular motors to control supramolecular polymerization processes and to form active nanostructures for the design of innovative materials.

Main

Molecular machines are (bio)chemical species capable of producing controlled mechanical motion to achieve a task. In cells, they support a number of key functions such as the synthesis of ATP, the translation of proteins, and the actuation of the cytoskeleton during muscular contraction.[1] Their actuation principles have been the subject of numerous debates,[2,3] and important achievements were made in the synthesis of artificial nanomachines over the past forty years.[4–13] The most advanced representants of molecular machines are molecular motors, which use power stroke and ratchet mechanisms as central concepts.[14,15] Conversely to molecular switches, which move their subparts back and forth between (meta)stable states, molecular motors exhibit the peculiar behaviour to generate a unidirectional, cyclic, and autonomous sequence of states when fuelled by an external source of energy.[16–18] This capacity to move out-of-equilibrium along a non-reciprocal spatial trajectory implies that molecular motors are able to progressively increase the work they deliver on their environment.[19–21] As prominent examples, Feringa's light-driven molecular motors rely on a series of alternating photoisomerization and thermal helix inversion (THI) steps to achieve a continuous unidirectional movement between a rotor and a stator linked together by a crowded carbon-carbon double bond (Figure 1a,b).[22,23] In a series of structural developments to decrease the THI activation barrier, Feringa designed a so-called "second generation" of molecular motors capable of producing very high rotation frequencies, up to the MHz regime in ideal conditions.[24] A recent line of intriguing studies have shown that the integration of these light-driven rotary motors into mechanical nanodevices and stimuli-responsive materials can push such systems out-of-equilibrium and even produce work up to the macroscopic scale.[25–27] In order to probe the capacity of such motors to rotate in a constrained environment,[28–32] we recently became interested by their potential incorporation into Langmuir layers. The Langmuir-Pockels trough provides a convenient method for the controlled formation and compression of 2D layers of amphiphilic molecules at the air-water interface, and the Langmuir-Blodgett technique allows to transfer these layers onto solid substrates.[33–35] Langmuir films with photoswitchable surfactants based on azobenzenes[36,37], spiropyrans[38,39], dithienylethenes[40], stilbenes[41] or overcrowded alkene switches[42] have been extensively studied and show differences in molecular packing, orientation, and surface pressures upon switching between two distinct configurational states. However, to the best of our knowledge, Langmuir layers were not built yet with advanced molecular motors in order to exploit their unique mechanical properties. In the present study, we show that the light-activation of amphiphilic molecular motors forming Langmuir monolayers can induce their unexpected nano- and microstructurations. We demonstrate that this phenomenon is the result of the motors' rotation that triggers an unprecedented type of supramolecular polymerization.[43–45]

Synthesis of amphiphilic motors

To access "motorized" Langmuir layers, we first designed two enantiopure amphiphilic rotary motors (**AM1** and **AM2**), which can autonomously rotate anticlockwise under UV light irradiation (**Figure 1a-c**).

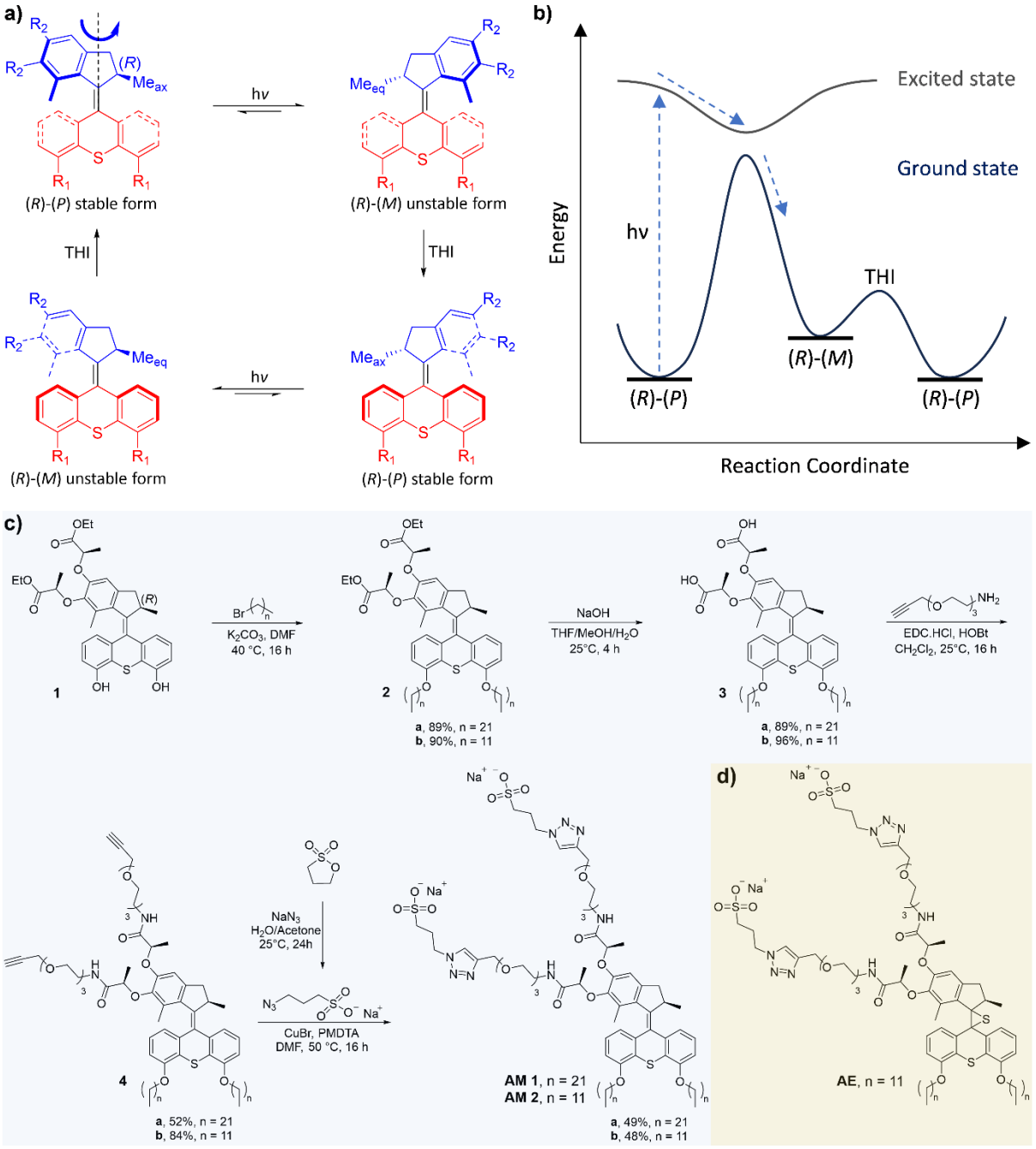

Figure 1. Molecular structures and corresponding chemical syntheses of key motorized amphiphiles investigated in this study. (**a**) The motor core is derivatized from 2nd generation Feringa's motors (with stator in red and rotor in blue), and capable of fast unidirectional 360° anticlockwise rotation around its double-bond axis at room temperature by following a non-reciprocal sequence comprised of two photoisomerizations and two thermal helix inversion (THI) processes (with frequencies reaching the MHz regime in ideal conditions).[24] (**b**) Corresponding energetic diagram describing a 180° rotation over 1 photochemical step and 1 thermal step. (**c**) Final steps of the synthetic route giving access to amphiphilic molecular rotary motors **AM1** and **AM2**. (**d**) Chemical structure of the "rotationally locked" amphiphilic episulfide **AE**.

We established a synthetic pathway starting from previously reported tetrasubstituted second generation Feringa's motor **1**,[25] followed by its derivation with a pair of hydrophobic alkyl chains on the stator part and a pair of hydrophilic chains on the rotor part (see supplementary information (SI) for all synthetic protocols and products characterization). **AM1** and **AM2** differ by the size of the linear alkyl chains attached to their thioxanthene moiety ($C_{22}H_{45}$, and $C_{12}H_{25}$, respectively). The final steps of this synthetic route start by the Williamson's etherification of the free phenol groups of motor **1** with 1-bromodocosane or 1-bromododecane to furnish with excellent yields intermediates **2a** and **2b**, respectively. After saponification of the (*R*)-lactic acid ethyl esters on the rotor part, and subsequent amidation with acetylene-triethyleneglycol-amine, compounds **4a,b** were engaged in a copper-catalysed Huisgen "click" reaction with intermediate **5** to introduce a pair of sodium sulphonate head groups. Overall, following this 4-step process, **AM1** was obtained with a total yield of 20%, and **AM2** with a total yield of 35% from **1**. An amphiphilic episulfide analogue (**AE**) was also prepared following the same synthetic pathway (Figure 1c). **AE** cannot rotate under UV activation and is used for control experiments in this study.

Formation of Langmuir layers

Langmuir films of pure molecules **AM1**, **AM2**, and **AE** were obtained by spreading their corresponding chloroform solution (c = 1 mg mL^{-1}) onto the air-water interface in a Langmuir trough at 25°C. The corresponding surface pressure – area isotherms are summarized in **Figure 2** (and Figure S1). The isotherms without UV irradiation (black curves) show the formation of well-condensed films for each amphiphile. Strikingly, direct UV light irradiation (365 nm, 1.86 $mW.cm^{-2}$) of the monolayers during the compression shifts the isotherms for motor amphiphiles **AM1** and **AM2** to smaller mean molecular areas (Figures 2a,b, and S1a,b, red curves). This behaviour seems counterintuitive at a first glance because one might expect that the rotational motion of the motors would lead to larger mean molecular areas on the interface. Therefore, we tried to analyse in more details the nature of this drop of the molecular area under light irradiation. First, the isotherm for **AM1** in the dark shows a plateau around 4.5 mN/m, characteristic of a phase transition reminiscent of lipid isotherms and a collapse area around 66 $Å^2$/molecule.[46–49] With UV irradiation, the plateau corresponding to the phase transition cannot be observed anymore and the collapse area is shifted to 52 $Å^2$/molecule. Second, the monolayer formed by **AM2** has a collapse area around 71 $Å^2$/molecule in the dark and its direct irradiation leads to a considerable shift of the isotherm to smaller molecular areas with a collapse area around 48 $Å^2$/molecule. Third, amphiphilic episulfide **AE** forms a monolayer with a collapse area around 73 $Å^2$/molecule in the dark (Figure 1c). However, direct UV irradiation of the episulfide layer does not lead to a detectable shift in the isotherm. In addition, repeating the isotherms for motor **AM2** and **AE** with slightly increased or decreased temperatures of the subphase does not significantly change the isotherms for both the irradiated and non-irradiated layers (Figure S2a and S2b). In addition, by monitoring the temperature of the Langmuir layer during light-irradiation with an infra-red thermometer, we could not detect variations higher than +/- 2°C (Figure S3). Hence, one can exclude from these control experiments that the shifts in the irradiated motorized monolayers arise from a photothermal effect.

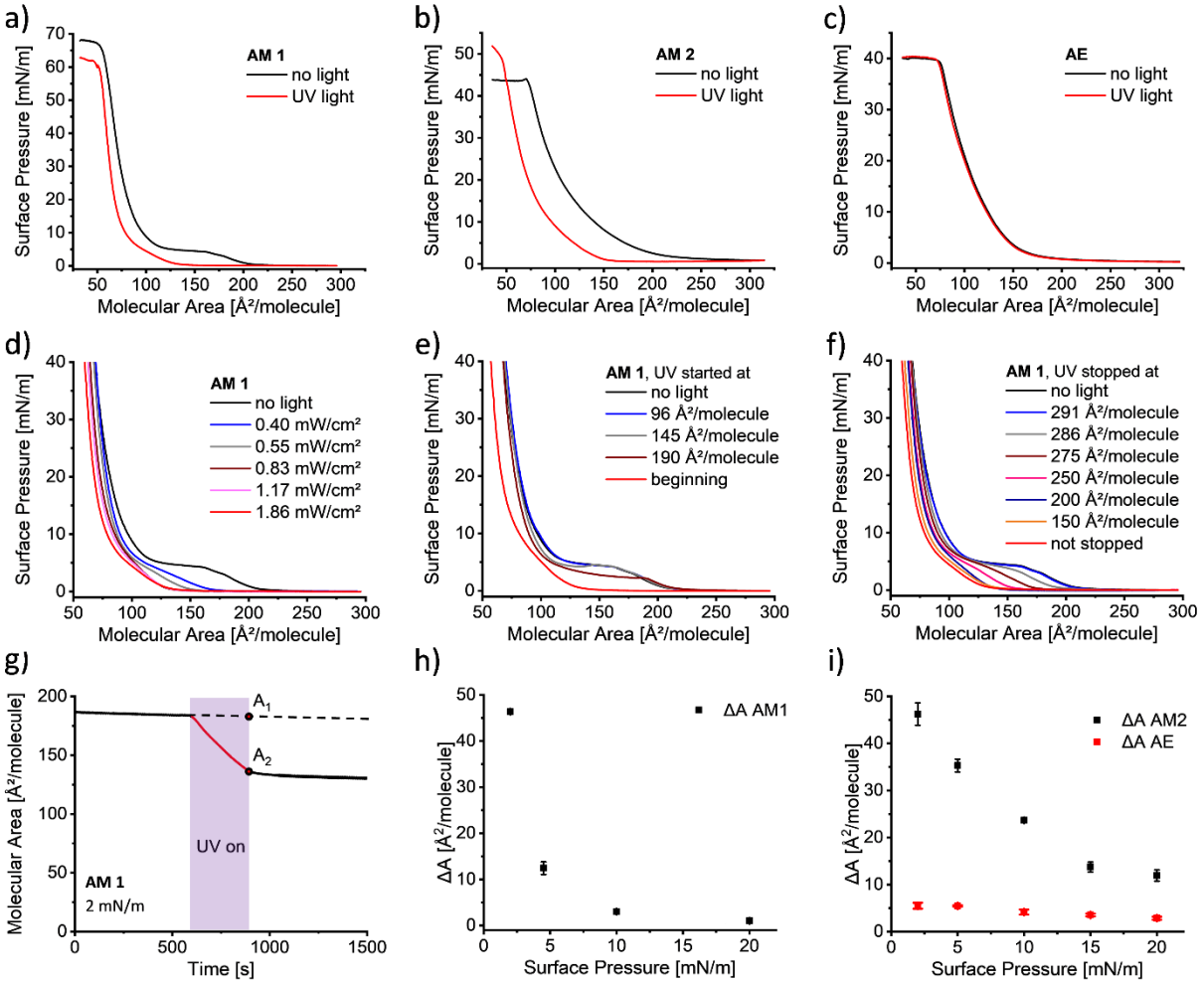

Figure 2. Formation and light-responsiveness of Langmuir monolayers made from motorized surfactants. (**a-c**) Surface pressure – molecular area isotherms of (**a**) **AM1**, (**b**) **AM2** and (**c**) **AE** on an ultrapure water surface (T = 25°C). Each plot contains a set of isotherms that represents Langmuir films prepared from the same stock solution (1 mg/mL) but under two different conditions: *i*) without light irradiation (black) and *ii*) with a direct irradiation of the water surface with UV light (365 nm, 1.86 $mW.cm^{-2}$) during the entire compression (red). (**d-f**) Surface pressure – molecular area isotherms of **AM1** (**d**) with variable UV light power intensities; (**e**) when the UV irradiation (365 nm, 1.86 $mW.cm^{-2}$) was started at different times after the beginning of the compression (*i.e.* 295.5 $Å^2$/molecule); and (**f**) when the UV irradiation (365 nm, 1.86 $mW.cm^{-2}$) was turned on at the beginning of the compression but stopped at different times during the compression. (**g**) Evolution of the molecular area over time under constant surface pressure at 2 mN/m for **AM1** before, during, and after UV light irradiation (for 5 minutes). Removing the area reached after stopping the UV irradiation (A_2) from the area of the extrapolation of the initial curve without irradiation at the intersection where the irradiation was stopped (A_1), represents the net effect of the 5 minutes-irradiation on the formed layers ($\Delta A = A_1 - A_2$) at a constant surface pressure. (**h**) ΔA values for **AM1**, representing the net effect of UV irradiation on the molecular area for different constant surface pressure values. (**i**) ΔA values for **AM2** and **AE** for different constant surface pressure values. The experiments were duplicated, with error bars showing the standard deviation.

To further investigate the impact of the direct UV irradiation, we varied the power of the LED light source, and observed that the films made of **AM1** and **AM2** are dependent on the intensity of the UV irradiation and therefore on the number of photons absorbed (Figure 2d and S2c). For a maximum power of 1.86 $mW.cm^{-2}$, the shifts in the compression isotherms are the highest, while they are less pronounced below 1 $mW.cm^{-2}$ (Figure 2d). In addition, we performed

experiments in which the irradiation was started or stopped at different times after starting the film compression. Starting the UV irradiation of **AM1** films at surface pressures above the phase transition does not lead to isotherm shifts while starting it at 2 or 4.5 mN/m results in smaller but noticeable shifts (Figure 2e). On the other hand, stopping the film irradiation as early as 275 Å^2/molecule (about 1 min of irradiation) shifts the rise in surface pressure to considerably smaller mean molecular areas (as compared to the non-irradiated case) accompanied by another important difference: the absence of a phase transition plateau (Figure 2f). The isotherms for **AM2** can be similarly shifted when the irradiation is started at surface pressures up to 20 mN/m (Figure S2d). While stopping the irradiation after reaching 150 Å^2/molecule leads to no difference in the isotherm compared to the fully irradiated isotherm (Figure S2e), stopping it earlier (above 150 Å^2/molecule) shifts the isotherms closer to the non-irradiated state. These results let us conclude that we can activate the motor layers at different stages before they become too compact, that is with a potential detrimental impact of the compression forces on the efficiency of the motor rotation. To better quantify this peculiar effect, we performed light irradiation experiments with constant surface pressures (Figure 2g). Important drops of the molecular area ($\Delta A = A_1 - A_2$) of **AM1** are observed for surface pressures up to 4.5 mN/m, whereas the effect of irradiation becomes negligible from the critical pressure of 10 mN.m^{-1} and above (Figure 2h). Furthermore, for films made of control episulfide **AE** the irradiation-induced shrinking remains negligible at any pressure, whereas this effect is pronounced for the shorter motorized analogue **AM2** even at 20 mN/m (Figure 2i). These experiments suggest that light-driven motors can rotate only for large enough molecular areas (lower enough surface pressures). We argue that from a certain threshold pressure imposed in the monolayer, the rotary motor becomes arrested by reaching its stall torque, and is not able to produce extra work to modify the Langmuir layer. This threshold value can be compared with the maximum torque delivered by this particular motor core, which was previously determined in the order of 10 pN.nm.[28] Very interestingly, it can be estimated that the size of a hypothetical blade attached to the motor to stop the rotation under the critical pressure (10 mN/m) corresponds to a typical length of ~ 1 nm, effectively in the order of the molecular motor's size (Figure S4 and corresponding discussion).

Supramolecular polymerization through motor's activation

We used the Langmuir-Blodgett (LB) technique to characterize the nature of the transferred films of **AM1** on solid substrates at different points of the non-irradiated and irradiated isotherms (Figures 3a and 3f). In particular, AFM was used to analyse the nano- and microstructures of the motorized monolayers on silicon wafers, revealing that LB films display unexpected and significantly original structural features when irradiated before deposition. For instance, films obtained at 2 and 10 mN/m in the dark show the formation of poorly structured aggregates (Figure 3b and 3c). Remarkably, the corresponding images of **AM1** at 2 and 10 mN/m, but being irradiated with UV light during the compression period, revealed that a monolayer is now composed of soft fibrillar structures which partially fuse side by side to create a 2D network (Figure 3g and 3h).

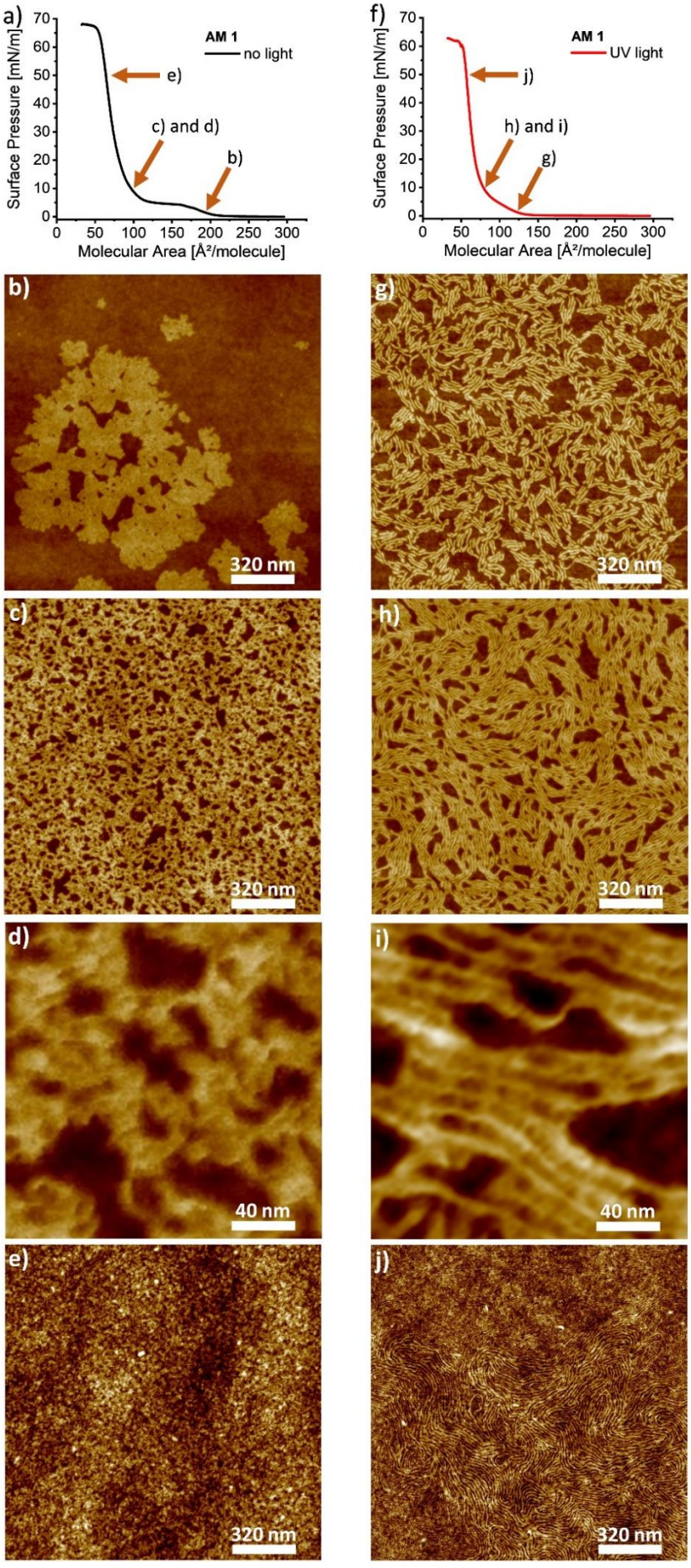

Figure 3. Microstructures of Langmuir monolayers made of motorized surfactants, without and with UV irradiation. (**a**,**f**) Surface pressure – molecular area isotherms of **AM 1**: (**a**) without and (**f**) with UV irradiation (365 nm, 1.86 mW) respectively. The arrows indicate at which compression the transfer of the film was done by the Langmuir-Blodgett technique. (**b-d**, **g-j**) AFM images of Langmuir-Blodgett films on silicon wafers of **AM 1** transferred at constant surface pressure: (**b**) 2 mN/m, without irradiation, (**c**) and (**d**) 10 mN/m, without irradiation and with different magnifications, (**e**) 50 mN/m without irradiation, (**g**) 2 mN/m, with UV irradiation (for 335 s), (**h**) and (**i**) 10 mN/m, with UV irradiation (for 630 s) and with different magnifications, (**j**) 50 mN/m with UV light irradiation (for 735 s). For irradiated films, the UV light was started from the beginning of the compression and turned off when the desired surface pressure was reached, followed by the transfer of the film.

Compression to 10 and 50 mN/m of the non-irradiated system gives a compact, aggregated film (Figure 3c and 3e), whereas at the same compression level the irradiated layer reveals a beautifully structured pattern made of defined fibrils (Figure 3h and 3j). Magnification of these fibrils (Figure 3i) show the side-by-side alignment of packed monodimensional objects with a diameter of ~ 3-5 nm (with a precision limited by the AFM tip convolution) and a lateral period of ~ 15 nm. These micrographs suggest that UV irradiation of a film of **AM1** leads to a linear supramolecular polymerization of the motorized amphiphiles at low surface pressures, followed by subsequent 2D morphing and lateral packing of these fibrils for higher compression values. To evaluate the effect of the compression on the fibril formation, we further investigated the potential initial structures formed before any compression, with a LB deposition of the non-irradiated surface layer at 295.5 $Å^2$/molecule (0 mN/m) (Figure S5). While patches of poorly defined aggregated structures were imaged for non-irradiated samples (Figure S5b), short fibrils of homogeneous diameters were revealed after 15 minutes of irradiation (365 nm, 1.86 mW/cm^2) (Figure S5c). The corresponding height profiles of these domains in the dark (Figure 4a) give a very regular thickness of 2.35 ± 0.15 nm above the silicon wafer, typically corresponding to a homogeneous monolayer. With UV irradiation these fibrils have a height of around 3.10 ± 0.19 nm, which presents an increase of ~ 32% compared to the non-irradiated domains. X-ray reflectometry (XRR) (Figure 4b) and height profiles from AFM measurements (Figure 4c and d) of samples at 4.5 mN/m also show an increase in height for the UV irradiated sample. The reflectivity spectra on Figure 4b presents clear Kiessig fringes, indicating that a layer has been deposited on the Si wafers substrate. The distances between the minima of the Kiessig fringes ΔQ is directly related to the overall thickness h of the deposited film via the expression

$$h = \frac{2\pi}{\Delta Q}$$

which is model independent and includes the native silicon oxide layer of the Si wafer. A direct proof that upon irradiation the amphiphilic layer compression leads to a remarkable molecular reorganization is the fact that for the irradiated sample (red circles, blue line), the width of the Kiessig fringe is shorter than for the non-irradiated one, indicating a thicker deposited layer. More precisely, the total thickness of the layer is 57 Å while for the non-irradiated one (black circles) it is 50 Å. Remarkably, the overall thickness for both irradiated and non-irradiated sample is less than 63 Å which is the theoretical length of the fully stretched amphiphilic molecule, implying the presence of a monolayer. Indeed, the spectra could only be fitted by using a single amphiphilic monolayer comprising of an internal bilayer structure (involving

hydrophilic and hydrophobic sublayers) on top of a buffer layer made by SiO_2 (see SI). The values for the total thickness of the layer derived from the fit

$$h_{total} = h_{SiO_2} + h_{hydrophilic} + h_{hydrophobic}$$

were 50 Å for the non-irradiated sample and 57 Å for the irradiated one, in agreement with the corresponding values of the ΔQ found by measuring the width of the Kiessig fringe. The thickness of the SiO_2 buffer layer from the fit was found to be 22.9 Å +/- 0.6 Å. As already observed qualitatively we find an increase of ~ 7Å in the amphiphilic monolayer height under UV irradiation in line with AFM data.

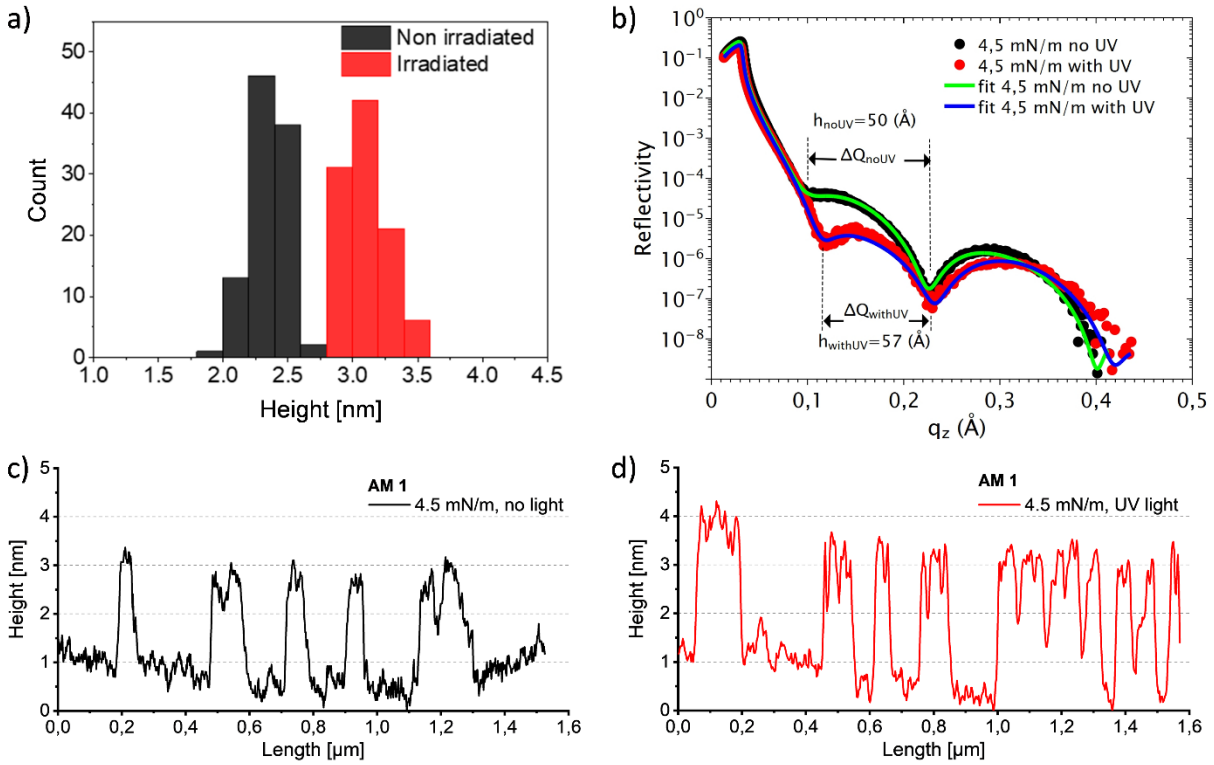

Figure 4. Thickness of Langmuir films. (**a**) Histogram of height measurements by AFM from Langmuir-Blodgett depositions at 295.5 $Å^2$/molecule without (black) and with previous UV irradiation for 15 minutes (red). (**b**) X-ray reflectometry (XRR) spectra with corresponding fits, of amphiphilic monolayers transferred on Si wafer substrates by the Langmuir Blodgett method at surface pressure of 4.5 mN/m (black circles) and at 4.5 mN/m under UV irradiation (red circles). The width of the characteristic Kiessig fringes is noted by ΔQ and is inversely proportional to the overal thickness of the layer. (**c-d**) Height profiles by AFM of selected sections of **AM1** LB films at 4.5 mN/m: (**c**) without irradiation, (**d**) with irradiation.

These results indicate that only light is necessary to generate linear supramolecular polymers, while the compression is only responsible for their further lateral packing, and that the height of the monolayer is influenced by light, but not really by the compression. Interestingly, Figure S6 shows an AFM image of a naked silicon wafer together with images of adhesion obtained from Figures S5b and c, showing important differences in adhesion between the silicon wafer and the formed structures, indicating that no further surfactants are present in between the structures. We also prepared LB film of **AM1** by first compressing the layer to 50 mN/m, and by then irradiating for 10 minutes the layer at the air-water interface under pressure control and

by finally depositing the film on the silicon surface (Figure S5d). The corresponding AFM image (Figure S5g) confirmed the absence of microstructuration, as in the case of the non-irradiated films, and as expected by the previous isotherms measured above a pressure of 10 mN/m (Figures 2e,h). In a reverse approach, isotherms were recorded for layers irradiated with UV light during 15 or 30 minutes at the open state (295.5 $Å^2$/molecule), followed by compression without irradiation (Figure S5e); showing that they resemble isotherms with UV irradiation during the entire compression. Furthermore, we prepared a LB film of **AM1** by irradiating the interface at the open state (295.5 $Å^2$/molecule) for 10 minutes, followed by resting in the dark for 2 hours (Figure S5f) and final deposition of the film at 50 mN/m, also revealing nano- and microstructurations (Figure S5h,i). This new set of experiments strongly suggest that differences in surface pressure result from the rotation of the motor in the low surface pressure regime (<10 mN/m) and from the subsequent molecular packing of the motorized surfactants in supramolecular polymers, leading to an apparent drop of the molecular area at constant compression values. The AFM images of **AM2** transferred at 30 mN/m without light irradiation also show non-organized films (Figure S7a). However, despite encouraging isotherms (Figure 2b), the LB films of **AM2** prepared at 30 mN/m with UV-light irradiation during the compression shows only additional aggregated structures with circular shapes but with no clear internal nanostructure (Figure S7b,c). NMR analysis of **AM2** irradiated in aqueous solution does not indicate degradation of the motor or cross-linking between the molecules (Figure S9). This suggests that the irradiation of **AM2** leads to the formation of densely packed amorphous aggregates, which can explain the shift in isotherms to smaller molecular areas, but with no evidence of supramolecular polymerization leading to well-organized patterns. We assume that attraction between **AM2** molecules with shorter alkyl tails is weaker, and that a loose amorphous structure is formed that densifies approaching equilibrium when exposed to UV irradiation. Hence, light-triggered supramolecular polymerization requires a fine balance between the different molecular parts of the motorized surfactants.

The mechanical stability and the potential structuration of the monolayer formed from **AM1** in the dark was then assessed by performing consecutive isotherm cycles under area control (Figure 5a) and under surface pressure control up to 50 mN/m (Figure 5b). The maximum surface pressure was very slightly dropped (Figure 5a) or shifted to smaller mean molecular areas (Figure 5b) after each cycle, indicating a small loss of material, possibly to the water subphase. However, the phase transition and the same overall shape of the isotherms can be observed for each cycle, which suggests that the formed layers are stable and reversible. AFM imaging of a transferred layer after 10 cycles under pressure control (Figure 5c) shows no significant difference by comparison with the film observed in Figure 3e. This result proves that the fibrils are formed under UV irradiation at low surface pressure, and cannot be obtained just after several compressions. In order to investigate if the initial isotherms can be recovered after UV irradiation and subsequent decompression, 3 cycles under area and pressure control were performed while the layers were irradiated with UV light during the second compression only, followed by decompression and relaxation for 15 h without irradiation (Figure 5d and 5e).

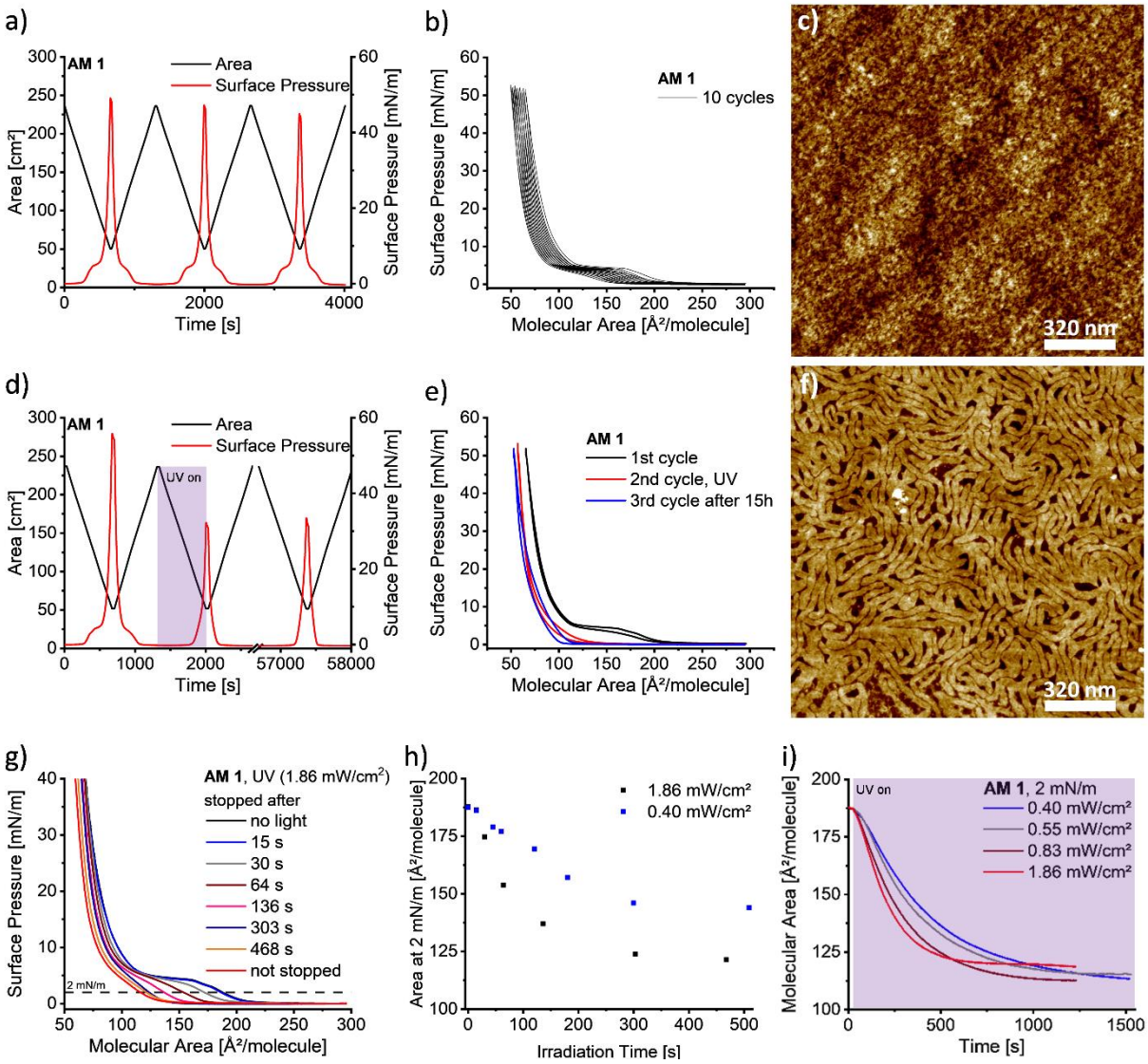

Figure 5. Multiple compressions of Langmuir monolayers made of motorized surfactants and study of the supramolecular growth mechanism. (**a**) Isotherm cycles of **AM1** under area control: 3 consecutive cycles without light irradiation. (**b**) Surface pressure – molecular area isotherms of **AM1** under pressure control: 10 consecutive cycles without light irradiation and (**c**) the corresponding AFM image of the final LB **AM1** film transferred at 50 mN/m after the 10th compression. (**d**) Surface pressure – molecular area isotherms of **AM1** under area control: 3 cycles with UV irradiation during the second compression only (violet background) and the third cycle performed 15h after the second decompression was completed. (**e**) Isotherm cycles of **AM1** under pressure control: 3 cycles with UV irradiation during the second compression only and a third cycle 15h after the second was performed. (**f**) AFM image of transferred LB films of **AM1** after compression to 50 mN/m under UV irradiation, followed by decompression and relaxation for 15h at the decompressed state without irradiation and recompression to 50 mN/m. (**g**) Surface pressure – molecular area isotherms of **AM1** where the UV irradiation (365 nm, 1.86 mW/cm^2) was stopped at different times after the beginning of the compression. (**h**) Molecular area at 2 mN/m plotted against the irradiation time from the beginning of the compression (cf. the corresponding cross-section points with the dashed line in (**g**)). (**i**) Evolution of the molecular area over irradiation time for **AM1** monolayers at 2 mN/m under surface pressure control, for various UV light intensities (the irradiation was started 30 seconds after the surface pressure of 2 mN/m was reached).

The system did not show a recovery of the initial isotherm nor the plateau of phase transition under the described conditions (cf. Fig. 5e). AFM imaging was performed for a layer that was first compressed to 50 mN/m under UV irradiation, decompressed and rested for 15h at the decompressed state without light and subsequently transferred at 50 mN/m. Much to our surprise, a strong thickening of the fibers could be revealed (Figures 5f, S8a), while keeping a constant height of 3 nm (Figure S8b) as observed for the initial fibrils (Figure 3j). This thickening results from lateral coagulation of several fibrils over time and is also obtained when the incubation time was extended to three days (Figure S8c). This suggests that the obtained supramolecular structures may be kinetically trapped by lateral coagulation perhaps due to better packing of alkyl tails explaining the irreversibility in the isotherms after UV irradiation.
We further investigated the growth mechanism for the supramolecular polymers formed by **AM1** at the interface by considering the time of irradiation from the start of the compression with different intensities of 1.86 mW/cm^2 and 0.40 mW/cm^2 (Figure 5g and S10). When plotting the molecular area at which a surface pressure of 2 mN/m was reached against the time of irradiation from the beginning of the compression, it can be observed that the smooth decrease in the area at short times is compatible with a parabolic law (Figure 5h). The absence of visible lag time suggests that a highly cooperative nucleation-growth mechanism should not rule the supramolecular polymerisation of these motor amphiphiles.[48,49] AFM images obtained for films irradiated during 30 seconds and 64 seconds after the start of the compression and transferred at 50 mN/m also show that, if some elongated structures are present (Figure S11a and b, respectively), the organisation of fully elongated structures is not observed as in Figure 3j taken as a reference (735 s of irradiation). These images further imply that the rotation of the motor is necessary for an extended period of time, and is necessary during the polymer growth, and not only at a nucleation stage as we would expect for a highly cooperative mechanism with kinetically facile elongation.[43] Further measurements at a constant surface pressure of 2 mN/m under pressure control with full-time irradiation but different UV light intensities display a similar short-time parabolic law, reaching plateaus with similar molecular area values in every case (Figure 5i). These results show that once the final state of the rearrangements is reached, the irradiation has no further influence on the monolayer of **AM1**.
To understand the correlations existing between the light-activation of the motor and the polymerization process, we investigated the UV and CD spectra of Langmuir layers made of **AM1**. Because **AM1** has a symmetric stator part (see blue part in Figure 1c), its *E* and *Z* stable isomers are degenerated ((*R*)-*P*-stable form), and the only differentiation existing between states in the rotary cycle takes place between the unstable ((*R*)-*M*) and the stable ((*R*)-*P*)) helix forms. We know that the life-time of the unstable helix in second generation Feringa's motors is very short at room temperature in solution (within the submicrosecond range),[24,25] but we tried to detect the presence of the unstable form in the monolayer, which could be kinetically trapped by compression or stacking of the motor. UV and CD analyses (that are adapted methods to differentiate between stable and unstable helical forms) can be compared. The absence of new peaks, sign inversion, or isobestic points indicates that both the non-organized layers (obtained in the dark) and the supramolecular polymers (obtained with light-irradiation) are formed from the stable helix only (Figure S12). Therefore, we conclude that, at the timescale of the film structuration, the motors are most of the time in their stable helix conformation, and that their supramolecular polymerization relies on their transient rotational activation during

light irradiation, and not on their dominant conformational state. This is coherent with other rotating systems incorporating second generation Feringa's motors, and in which the unstable helix cannot be observed at room temperature, even in very constrained conditions.[28,30,32] Putting together the experimental results described above, we propose a simplified mechanism of the entire supramolecular polymerization process at work in these motorized Langmuir layers (Figure 6), which is further supported by a theoretical model discussed in the SI (section S4).

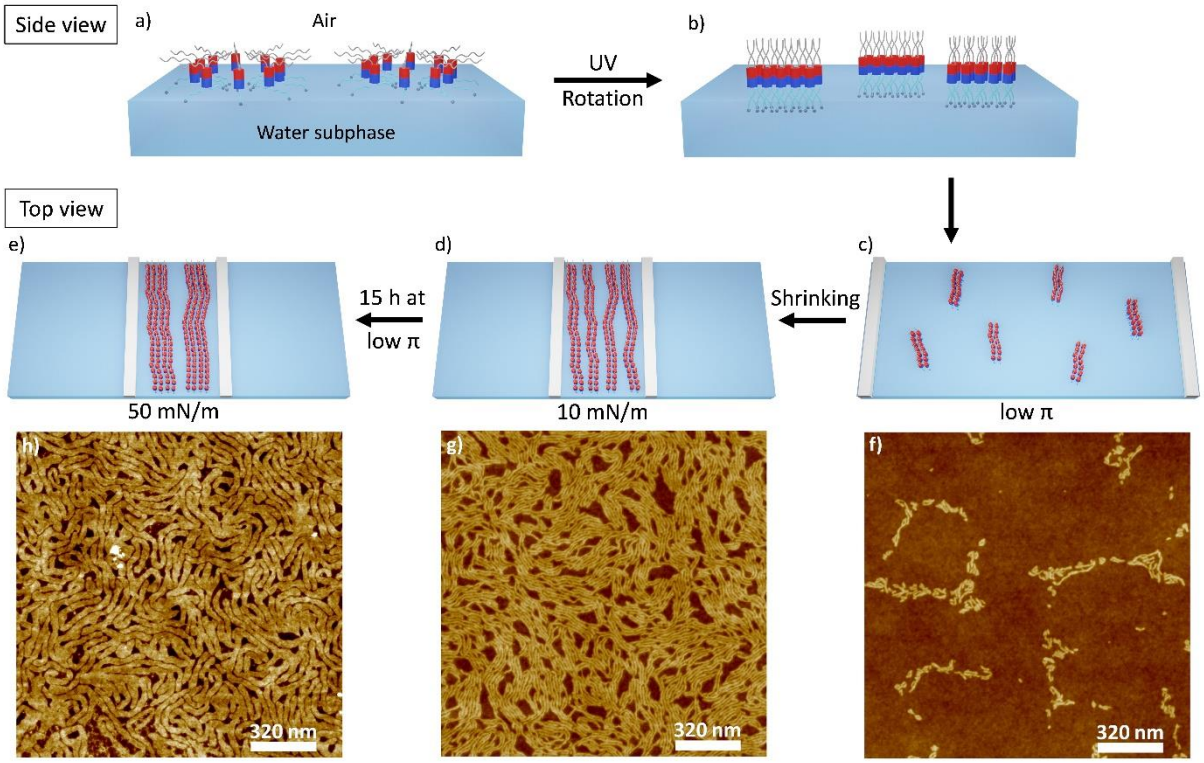

Figure 6. Proposed mechanism of the UV-driven supramolecular polymerization of motorized amphiphiles AM1 taking place within Langmuir monolayers. The first row (**a**,**b**) of sketches represents states with large molecular areas, followed by the layer compression (the second row of sketches (**c**-**e**)) accompanied with lateral spatial organization of the formed fibers, with the corresponding AFM images shown below (**f**-**h**).

For large mean molecular areas, **AM1** is condensed in poorly organized islands that further aggregate when compressing the layer to give a stable film of ~ 2.35 nm thickness. In addition to the amorphous material, the proposed theoretical model predicts that these islands and films can contain a certain proportion of small ring-like structures based on the isotactic π-π stacking between the aromatic cores of the motor with intrinsic curvature. During the irradiation process, the rotation of **AM1** can transiently modify its conformation in the ~1 Hz regime and provides sufficient activation energy (~ 125 k_BT) to break these rings, which can recombine differently – with a high gain of interfacial energy (~ 70 k_BT) – into rigid double columnar stacks composed of two fibrils with opposite intrinsic curvatures. These stretched double columnar stacks with an increased thickness of ~ 3.10 nm (+0.7nm) can then grow by merging with other double columnar stacks or by further association of supplementary unimers coming from amorphous material, explaining the requirement of UV irradiation all along the supramolecular polymerization. The length of these supramolecular polymers is therefore concentration

dependent, increasing during compression, while their thickening is induced by lateral coagulation of several linear fibres.

Conclusion

The present article reports on the first example of a supramolecular polymerization induced by the unidirectional rotation of molecular motors. The mechanistic control over supramolecular polymerization processes has become an important topic in modern chemistry, with the objective to access entirely new classes of stimuli-responsive, adaptive, and even "life-like" soft materials.[50] By making supramolecular polymers from active molecular motors, we have shown that one can shape their structure and modify their dynamics of growth by playing with the autonomous out-of-equilibrium motion of their monomers, provided the system is fuelled with an appropriate source of energy – here photons, but red-ox or chemical fuels can also be envisioned with other motors. The present self-assembly mechanism, limited by the stall torque of the motor (~ 10 pN.nm), is profoundly different from those involving molecular switches that can influence polymer structures by flipping between their different states. Here, on average, the motors stay in their unique stable state, and the emergence and growth of well-defined nanostructures is caused by work produced via jump-like unidirectional rotation of the motors under the action of light. We are now actively pursuing our investigations to access 3D motorized supramolecular polymers in the bulk solvent.

Acknowledgements

This work was granted by the European Commission's Horizon 2020 Programme as part of the MSCA-ITN project ArtMoMa under grant no. 860434. The authors are deeply grateful to the CEA-Saclay and A. Chenneviere for his help during the XRR experiments. This work was also supported by the Agence Nationale pour la Recherche (Grant number MONA_LISA ANR-20-CE09-0012, fellowships to A.C. and I.N.). The authors wish to acknowledge the Centre National de la Recherche Scientifique (CNRS), the University of Strasbourg, the University Paris Cité, and the Institut Universitaire de France.

Author contributions

N.G. and J.M.L. conceived the project. P.S. and D.D. synthesized the motor amphiphiles. P.S. performed all the Langmuir layers experiments with the help of L.A.A.. M.M. performed the AFM experiments. I.N. and A.S. developed the theoretical model. A.C. and E.B. performed and analysed the reflectometry experiments. N.G. directed the research with the help of E.M. who contributed to analyse all the data. P.S. and N.G. wrote the paper with input from all authors.

Competing interests

Authors declare that they have no competing interests.

Data and materials availability

Original data can be obtained from corresponding authors upon reasonable request.

Supplementary Materials

Synthetic protocols and characterization of synthesized compounds; their corresponding ^{1}H and $^{13}CNMR$ spectra; Langmuir films preparation and irradiation procedures; supplementary data on isotherms, AFM, and reflectometry experiments; theoretical model of the motorized supramolecular polymerization process.

References

1. Schliwa, M. & Woehlke, G. Molecular motors. *Nature* **422**, 759–765 (2003).
2. Jülicher, F., Ajdari, A. & Prost, J. Modeling molecular motors. *Rev. Mod. Phys.* **69**, 1269–1282 (1997).
3. Astumian, R. D. How molecular motors work – insights from the molecular machinist's toolbox: the Nobel prize in Chemistry 2016. *Chem. Sci.* **8**, 840–845 (2017).
4. Sauvage, J.-P. From Chemical Topology to Molecular Machines (Nobel Lecture). *Angew. Chem. Int. Ed.* **56**, 11080–11093 (2017).
5. Stoddart, J. F. Mechanically Interlocked Molecules (MIMs)-Molecular Shuttles, Switches, and Machines (Nobel Lecture). *Angew. Chem. Int. Ed.* **56**, 11094–11125 (2017).
6. Feringa, B. L. The Art of Building Small: From Molecular Switches to Motors (Nobel Lecture). *Angew. Chem. Int. Ed.* **56**, 11060–11078 (2017).
7. Leigh, D. A., Wong, J. K. Y., Dehez, F. & Zerbetto, F. Unidirectional rotation in a mechanically interlocked molecular rotor. *Nature* **424**, 174–179 (2003).
8. Ragazzon, G., Baroncini, M., Silvi, S., Venturi, M. & Credi, A. Light-powered autonomous and directional molecular motion of a dissipative self-assembling system. *Nat. Nanotechnol.* **10**, 70–75 (2015).
9. Guentner, M. *et al.* Sunlight-powered kHz rotation of a hemithioindigo-based molecular motor. *Nat. Commun.* **6**, 8406 (2015).
10. Cheng, C. *et al.* An artificial molecular pump. *Nat. Nanotechnol.* **10**, 547–553 (2015).
11. Borsley, S., Kreidt, E., Leigh, D. A. & Roberts, B. M. W. Autonomous fuelled directional rotation about a covalent single bond. *Nature* **604**, 80–85 (2022).
12. Pumm, A.-K. *et al.* A DNA origami rotary ratchet motor. *Nature* **607**, 492–498 (2022).
13. Zhang, L. *et al.* An electric molecular motor. *Nature* **613**, 280–286 (2023).
14. Borsley, S., Leigh, D. & Roberts, B. M. W. Molecular Ratchets and Kinetic Asymmetry: Giving Chemistry Direction. *Angew. Chem. Int. Ed.* DOI: 10.1002/anie.202400495 (2024) doi:10.1002/anie.202400495.
15. Astumian, R. D. Kinetic Asymmetry and Directionality of Nonequilibrium Molecular Systems. *Angew. Chem. Int. Ed.* **63**, (2024).
16. Erbas-Cakmak, S., Leigh, D. A., McTernan, C. T. & Nussbaumer, A. L. Artificial Molecular Machines. *Chem. Rev.* **115**, 10081–10206 (2015).
17. Feng, Y. *et al.* Molecular Pumps and Motors. *J. Am. Chem. Soc.* **143**, 5569–5591 (2021).
18. Baroncini, M., Silvi, S. & Credi, A. Photo- and Redox-Driven Artificial Molecular Motors. *Chem. Rev.* **120**, 200–268 (2020).
19. Dattler, D. *et al.* Design of Collective Motions from Synthetic Molecular Switches, Rotors, and Motors. *Chem. Rev.* **120**, 310–433 (2020).
20. Moulin, E., Faour, L., Carmona-Vargas, C. C. & Giuseppone, N. From Molecular Machines to Stimuli-Responsive Materials. *Adv. Mater.* **32**, 1906036 (2020).
21. Perrot, A., Moulin, E. & Giuseppone, N. Extraction of mechanical work from stimuli-

responsive molecular systems and materials. *Trends Chem.* **3**, 926–942 (2021).
22. Koumura, N., Zijlstra, R. W. J., van Delden, R. A., Harada, N. & Feringa, B. L. Light-driven monodirectional molecular rotor. *Nature* **401**, 152–155 (1999).
23. Pooler, D. R. S., Lubbe, A. S., Crespi, S. & Feringa, B. L. Designing light-driven rotary molecular motors. *Chem. Sci.* **12**, 14964–14986 (2021).
24. Koumura, N., Geertsema, E. M., van Gelder, M. B., Meetsma, A. & Feringa, B. L. Second Generation Light-Driven Molecular Motors. Unidirectional Rotation Controlled by a Single Stereogenic Center with Near-Perfect Photoequilibria and Acceleration of the Speed of Rotation by Structural Modification. *J. Am. Chem. Soc.* **124**, 5037–5051 (2002).
25. Li, Q. *et al.* Macroscopic contraction of a gel induced by the integrated motion of light-driven molecular motors. *Nat. Nanotechnol.* **10**, 161–165 (2015).
26. Foy, J. T. *et al.* Dual-light control of nanomachines that integrate motor and modulator subunits. *Nat. Nanotechnol.* **12**, 540–545 (2017).
27. Perrot, A., Wang, W., Buhler, E., Moulin, E. & Giuseppone, N. Bending Actuation of Hydrogels through Rotation of Light-Driven Molecular Motors. *Angew. Chem. Int. Ed.* **62**, e202300263 (2023).
28. Gao, C., Vargas Jentzsch, A., Moulin, E. & Giuseppone, N. Light-Driven Molecular Whirligig. *J. Am. Chem. Soc.* **144**, 9845–9852 (2022).
29. García-López, V. *et al.* Molecular machines open cell membranes. *Nature* **548**, 567–572 (2017).
30. Wang, W.-Z. *et al.* Light-Driven Molecular Motors Boost the Selective Transport of Alkali Metal Ions through Phospholipid Bilayers. *J. Am. Chem. Soc.* **143**, 15653–15660 (2021).
31. Qutbuddin, Y. *et al.* Light-Activated Synthetic Rotary Motors in Lipid Membranes Induce Shape Changes Through Membrane Expansion. *Adv. Mater.* DOI: 10.1002/adma.202311176 (2024) doi:10.1002/adma.202311176.
32. Daou, D. *et al.* Out-of-Equilibrium Mechanical Disruption of β-Amyloid-Like Fibers using Light-Driven Molecular Motors. *Adv. Mater.* DOI: 10.1002/adma.202311293 (2024) doi:10.1002/adma.202311293.
33. Ariga, K., Yamauchi, Y., Mori, T. & Hill, J. P. 25th Anniversary Article: What Can Be Done with the Langmuir-Blodgett Method? Recent Developments and its Critical Role in Materials Science. *Adv. Mater.* **25**, 6477–6512 (2013).
34. Oliveira, O. N., Caseli, L. & Ariga, K. The Past and the Future of Langmuir and Langmuir–Blodgett Films. *Chem. Rev.* **122**, 6459–6513 (2022).
35. Ariga, K. Don't Forget Langmuir–Blodgett Films 2020: Interfacial Nanoarchitectonics with Molecules, Materials, and Living Objects. *Langmuir* **36**, 7158–7180 (2020).
36. Kim, I., Rabolt, J. F. & Stroeve, P. Dynamic monolayer behavior of a photo-responsive azobenzene surfactant. *Colloids Surfaces A Physicochem. Eng. Asp.* **171**, 167–174 (2000).
37. Backus, E. H. G., Kuiper, J. M., Engberts, J. B. F. N., Poolman, B. & Bonn, M. Reversible Optical Control of Monolayers on Water through Photoswitchable Lipids. *J. Phys. Chem. B* **115**, 2294–2302 (2011).
38. Ando, E., Miyazaki, J., Morimoto, K., Nakahara, H. & Fukuda, K. J-aggregation of photochromic spiropyran in Langmuir-Blodgett films. *Thin Solid Films* **133**, 21–28 (1985).
39. Nakazawa, T., Azumi, R., Sakai, H., Abe, M. & Matsumoto, M. Brewster Angle Microscopic Observations of the Langmuir Films of Amphiphilic Spiropyran during Compression and under UV Illumination. *Langmuir* **20**, 5439–5444 (2004).
40. Rossos, A. K. *et al.* Photochromism of Amphiphilic Dithienylethenes as Langmuir–

Schaefer Films. *Langmuir* **34**, 10905–10912 (2018).
41. Karthaus, O., Shimomura, M., Hioki, M., Tahara, R. & Nakamura, H. Reversible Photomorphism in Surface Monolayers. *J. Am. Chem. Soc.* **118**, 9174–9175 (1996).
42. Cheng, J., Štacko, P., Rudolf, P., Gengler, R. Y. N. & Feringa, B. L. Bidirectional Photomodulation of Surface Tension in Langmuir Films. *Angew. Chem. Int. Ed.* **56**, 291–296 (2017).
43. De Greef, T. F. A. *et al.* Supramolecular Polymerization. *Chem. Rev.* **109**, 5687–5754 (2009).
44. Aida, T., Meijer, E. W. & Stupp, S. I. Functional Supramolecular Polymers. *Science (80-.).* **335**, 813–817 (2012).
45. Roy, N., Schädler, V. & Lehn, J.-M. Supramolecular Polymers: Inherently Dynamic Materials. *Acc. Chem. Res.* **57**, 349–361 (2024).
46. Luviano, A. S., Campos-Terán, J., Langevin, D., Castillo, R. & Espinosa, G. Mechanical Properties of DPPC–POPE Mixed Langmuir Monolayers. *Langmuir* **35**, 16734–16744 (2019).
47. Pallas, N. R. & Pethica, B. A. Liquid-expanded to liquid-condensed transition in lipid monolayers at the air/water interface. *Langmuir* **1**, 509–513 (1985).
48. Davies, J. T. & Rideal, E. K. *Interfacial Phenomena*. (Academic Press, London, 1963).
49. Dervichian, D. G. Changes of Phase and Transformations of Higher Order in Monolayers. *J. Chem. Phys.* **7**, 931–948 (1939).
50. *Out-of-Equilibrium (Supra)molecular Systems and Materials*. (Wiley, 2021). doi:10.1002/9783527821990.

Graphical abstract for TOC

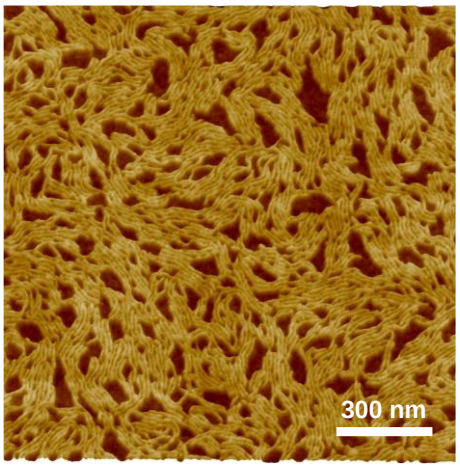

Supramolecular morphing using molecular motors. An amphiphilic light-driven rotary motor is used as a surfactant to form Langmuir monolayers at the air-water interface. Upon UV irradiation, the work produced by the continuous unidirectional rotation of the motor can trigger its supramolecular polymerization and the subsequent patterning of its interfacial layer at the nanoscale.